ACS OMEGA

http://pubs.acs.org/journal/acsodf

Article

Analysis and Comparison of Mouse and Human Brain Gangliosides via Two-Stage Matching of MS/MS Spectra

Fanran Huang, Laura S. Bailey, Tianqi Gao, Wenjie Jiang, Lei Yu, David A. Bennett, Jinying Zhao, Kari B. Basso, and Zhongwu Guo*

Cite This: *ACS Omega* 2022, 7, 6403−6411

Read Online

ACCESS | Metrics & More | Article Recommendations | Supporting Information

ABSTRACT: Glycosphingolipids (GSLs), including gangliosides, are essential components of the cell membrane. Because of their vital biological functions, a facile method for the analysis and comparison of GSLs in biological issues is desired. To this end, a new method for GSL analysis was developed based on two-stage matching of the carbohydrate and glycolipid product ions of experimental and reference MS/MS spectra of GSLs. The applicability of this method to the analysis of gangliosides in biological tissues was verified using human plasma and mouse brains spiked with standards. The method was then used to characterize endogenous gangliosides in mouse and human brains. It was shown that each endogenous ganglioside species had varied lipid forms and that mouse and human brains had different compositions of ganglioside species and lipid forms. Moreover, a 36-carbon ceramide is found to represent the major lipid form for mouse brain gangliosides, while the major lipid form for most human brain gangliosides is a 38-carbon ceramide. This study has verified that the two-stage MS/MS spectral matching method could be used to study gangliosides or GSLs and their lipid forms in complex biological samples, thereby having a broad application.

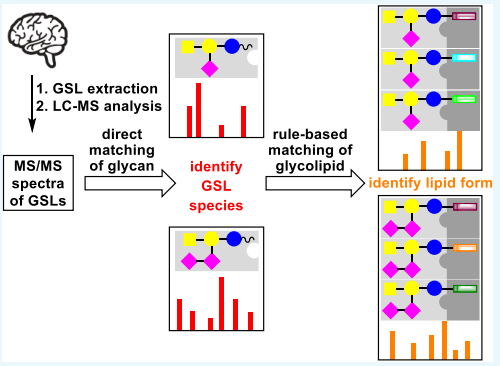

INTRODUCTION

Glycosphingolipids (GSLs) are a family of complex glycolipids having hydrophilic glycans attached to hydrophobic ceramides via a glycosidic bond.[1,2] As an essential component of the cell membrane, GSL is ubiquitous and especially rich in the human central nervous system (CNS), such as brain,[3−5] to play a vital role in signal transduction, neuronal cell recovery, differentiation, and memory.[6−11] GSLs are also involved in many pathological conditions,[12−14] such as cancer,[15,16] Alzheimer's disease,[17−21] and various storage disorders.[22,23] Therefore, information about the compositions of GSLs in human tissues is fundamental for understanding their biological functions.

The structures of GSLs are very complex and diverse, with variations in both the glycan and the lipid, making their analysis challenging. To address this issue, tandem mass spectrometry (MS/MS or MS^n), which can offer detailed structural information, has been widely used for GSL characterization and glycolipidomics analysis. In addition, MS is usually coupled with chromatography[24−38] to tackle issues such as isobaric overlap, isomer separation, and ion suppression on GSL species of low abundance. Meanwhile, new MS technologies, *e.g.*, ion mobility spectrometry-mass spectrometry (IMS-MS), are explored to further improve ion differentiation.[39,40] The most commonly used ionization method has been electrospray ionization (ESI),[41,42] due to its mild condition to afford intact precursor ions of GSLs and its ease to couple with various chromatographic techniques. Overall, ESI liquid chromatography (LC)-MS^n proves to be a powerful tool for the analysis and quantitation of GSLs.

Despite these progresses, GSL analysis remains difficult. In contrast to glycoproteins, where proteins and glycans can be cleaved and studied individually,[43] GSLs are analyzed intact. The complex and diverse glycoforms and lipid forms of GSLs not only make their analysis challenging but also hamper the application of methods developed for glycomics and lipidomics analysis. Furthermore, presently, there is a lack of an extensive database of reference MS/MS spectra for GSL identification and a software especially designed for comprehensive GSL analysis.

To address the problem, our labs have recently explored a novel LC-MS/MS-based strategy for GSL characterization.[44] It has been shown that MS bond cleavage of GSLs occurs mainly to glycan to form two types of product ions, namely, "carbohydrate product ions"—fragments containing only carbohydrates—and "glycolipid product ions"—fragments containing both the carbohydrates and the lipid.[44,45] Moreover, different lipid forms of a GSL species do not have a significant

Received: December 14, 2021
Accepted: January 28, 2022
Published: February 10, 2022

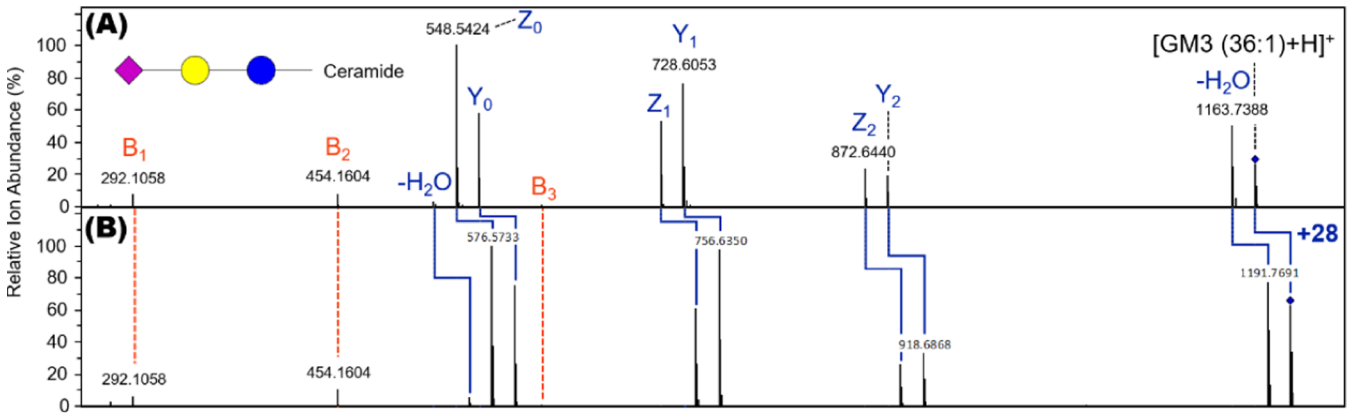

Figure 1. MS/MS spectra and product ions of (A) GM3 (36:1) and (B) GM3 (38:1) by CID of the protonated precursor ions (blue diamonds). Panel (A) also contains a depiction of GM3 structure and product ion labels. The dashed orange lines highlight fragments appearing at the same *m/z* in both spectra. The solid blue lines highlight fragments that increase in mass from (A) to (B) spectra due to different lipid structures.

impact on its glycan dissociation pattern. Thus, for any GSL species, carbohydrate product ions are conserved regardless of the lipid form, and the ion masses of glycolipid product ions may shift by a constant number due to changes in the lipid structure, while the spectral pattern (*e.g.*, the mass separation and peak intensities) remains unchanged. Accordingly, GSLs can be characterized in two steps. First, after the MS/MS spectrum of an experimental GSL is obtained, its carbohydrate product ions are matched with those of reference MS/MS spectra in the database. This will directly characterize the glycan structure, which defines the GSL species. Next, the rule-based method[46−48] is employed to match the glycolipid product ions of the experimental and reference spectra. This will characterize the ceramide structure, which defines the lipid form of a GSL. As a positive identification is made only after both carbohydrate and glycolipid product ions of the experimental and reference spectra are matched, the new method can minimize the risk of false characterization. In addition, the application of rule-based matching in the second stage makes it possible to identify various lipid forms of a GSL species in the presence of only one reference spectrum in any lipid form. Therefore, this method will facilitate GSL analysis using a reduced database, *i.e.*, containing only one reference spectrum for each GSL species.

In the previous paper,[44] we reported a proof-of-concept study on the new two-stage matching method using standard samples. As the ultimate goal of this method is its application to studying GSL profiles and glycolipidomics in biological tissues, in this endeavor, we embarked on probing it with biological samples and exploring ganglioside compositions in mouse and human brains.

RESULTS AND DISCUSSION

We planned to verify first that the two-stage MS/MS spectral matching method would be practical for GSL characterization and glycolipidomics analysis of biological tissues using well-defined samples. In this regard, we generated some GSL-spiked plasma and brain tissues utilizing commercial GSL standards and subjected them to extraction and LC-MS/MS studies. This also served to validate if our extraction protocol was effective in retrieving all GSLs. Finally, the extraction protocol and LC-MS conditions were applied to mouse and human brain GSL analysis. Here, we were expressly focused on gangliosides—a sialylated subgroup of GSL—limited by the scope of our reference library.

For GSL identification, currently, there is no software especially designed for the two-stage matching of experimental and reference MS/MS spectra. We employed two existing software-based approaches to address this problem. One approach utilized Metaboscape (Bruker, v5) to assist the first matching stage. The reference carbohydrate ions of each GSL species were searched among the experimental data using Metaboscape, with a search window of calculated mass ± one mass unit, to generate a list of potential precursor ions. The second matching stage was performed manually using the much-reduced precursor ion list. To this end, the unit mass difference between experimental and reference precursors was calculated and applied to all glycolipid product ions in the reference MS/MS spectrum to generate a rule-based reference spectrum. This was then compared with the experimental product spectrum to determine the lipid form. Finally, the experimental and reference spectra were manually compared to further verify the results. Only if all carbohydrate and glycolipid product ions matched with an error <20 ppm was a GSL positively identified.

Another approach makes use of Compass Analysis software. First, the precursor masses for various lipid forms of each ganglioside were calculated by adding or subtracting 2, 4, 26, 28, 30, 54, 56, 58, etc., mass units to or from the reference. These represent lipid forms of different saturation patterns and chain lengths, but we understand that this approach cannot be exhaustive. Then, experimental data were extracted using Compass Analysis software to obtain a list of possible precursors matching the calculated masses. Finally, the identified precursors were subjected to a two-stage analysis of the MS/MS data as above. Similarly, only if all carbohydrate and glycolipid product ions matched was a positive identification made. Both approaches above were tested and gave similar results.

Analysis of Spiked Human Plasma. Ganglioside-spiked plasma used in this study was generated by mixing human plasma with GM3, GM2, and GM1 standards, as described in the Experimental Method section. Thereafter, gangliosides in the spiked plasma were extracted with a 3:4:2 mixture of water, methanol, and chloroform, referring to a reported protocol.[49] The extracts were dried and then reconstituted in methanol containing 1% chloroform before being subjected to LC-MS/

https://doi.org/10.1021/acsomega.1c07070
ACS Omega 2022, 7, 6403−6411

MS analysis under conditions described in the Experimental Methods section. Finally, the MS/MS spectra from each sample were analyzed by the above-described two-stage matching method.

The MS/MS spectrum of GM3, which carries a rather simple trisaccharide (Figure 1A), has three prominent carbohydrate product ions, all being B-type ions (B_1, B_2, and B_3 ions at m/z 292.1027, 454.1555, and 616.2083, respectively), and eight glycolipid product ions (Z_0, Z_0-H_2O, Y_0, Z_1, Y_1, Z_2, Y_2, and M-H_2O ions). As glycosidic bonds in GSLs are the most fragile and prone to cleavages, understandably, GM3, like other GSLs, gives mainly B-type ions and the low intensities of C-type ions.

The first-stage matching of the experimental MS/MS spectra of spiked plasma with carbohydrate product ions of reference GM3 yielded a subset of precursors that contained all three B-type ions. Their MS/MS spectra were then subjected to rule-based matching with eight glycolipid product ions (Y, Z, Z-H_2O, and M-H_2O ions). This resulted in five precursor ions containing all desired product ions. They were finally identified as various lipid forms of GM3, *i.e.*, (34:1), (36:1), (38:1), (40:1), and (42:1) at m/z 1153.7205, 1181.7537, 1209.7871, 1237.8141, and 1265.8426 (Table 1), respectively. These

Table 1. Major Ganglioside Species and Their Lipid Forms Identified in Spiked Plasma

LC RT (min)	experimental m/z	theoretical m/z	mass deviation (ppm)	ganglioside ID
25.2	1153.72045	1153.7204	0.04	GM3 (34:1)
28.7	1181.7537	1181.7517	1.69	GM3 (36:1)
32.0	1209.7871	1209.7830	3.39	GM3 (38:1)
34.5	1237.8141	1237.8143	−0.16	GM3 (40:1)
37.5	1265.8426	1265.8456	−2.37	GM3 (42:1)
27.9	1384.8303	1384.8310	−0.51	GM2 (36:1)
31.1	1412.8640	1412.8623	1.20	GM2 (38:1)
27.1	1546.8772	1546.8839	−4.33	GM1 (36:1)
30.1	1574.9087	1574.9152	−4.13	GM1 (38:1)

results agreed with that of our previous studies on standard GM3.[44] The MS/MS spectra of GM3 lipid forms and their ion peaks and intensities are presented in the Supporting Information (Figure S4 and Table S1).

Next, the more complicated GM2 and GM1 were identified from spiked plasma by the same method. For the first stage of matching with GM2, the reference carbohydrate product ions were B_{1a}, B_2Y_{2a}, B_2Y_{2b}, B_3Y_{2a}, B_2, C_2, and B_3. For GM1, they were B_{1b}, B_{2a}, B_3Y_{2a}, B_3Y_{2b}, B_3Y_{3a}, B_3, and B_4. During the second stage of matching, the reference glycolipid product ions used to characterize the lipid forms of GM2 were Z_0, Y_0, Z_1, Y_1, $Y_{2b}Z_{2a}$, $Y_{2a}Y_{2b}$, Z_{2a}, Y_{2a}, Z_{2b}, Y_{2b}, and M-H_2O; for GM1, they were Z_0, Y_0, Z_1, Y_1, $Y_{2a}Z_{2b}$, $Y_{2b}Y_{2a}$, Y_{2a}, Y_{2b}, Y_{3a}, and M-H_2O. Finally, two GM2 lipid forms, (36:1) and (38:1), and two GM1 lipid forms, (36:1) and (38:1), were identified (Table 1). Their MS/MS spectra and product ions and intensities are presented in the Supporting Information (Figures S5, S6 and Tables S2, S3).

The results revealed that various gangliosides, including their different lipid forms, were successfully extracted from spiked human plasma and identified. Thus, the protocol to extract gangliosides from plasma using a 3:4:2 mixture of water, methanol, and chloroform was efficient for GSLs with different glycans. Importantly, the results proved that LC-MS combined with the two-stage matching of reference and experimental MS/MS spectra could be used to analyze GSLs in plasma.

Analysis of Spiked Mouse Brain. The brain is more complex and difficult to analyze than plasma as the former is heterogeneous and contains lipids and other membrane components that may interfere with GSL extraction and analysis. To validate the above extraction protocol and LC-MS conditions, first, we applied them to the study of defined brain samples. To this end, we generated ganglioside-spiked brain tissues by homogenizing GM3, GM2, and GM1 standards with the mouse brain. The spiked tissues were subjected to extraction, sample processing, and LC-MS/MS analysis as described.

The two-stage matching of LC-MS/MS spectra from spiked brain samples with reference spectra of GM3, GM2, and GM1 resulted in the identification of all spiked gangliosides in various lipid forms (Table 2). For example, four lipid forms of

Table 2. Major Ganglioside Species and Their Lipid Forms Identified in the Spiked Mouse Brain

LC RT (min)	experimental m/z	theoretical m/z	mass deviation (ppm)	ganglioside ID
25.6	1153.7195	1153.7204	−0.78	GM3 (34:1)
28.3	1181.7531	1181.7517	1.18	GM3 (36:1)
30.1	1209.7849	1209.7830	1.57	GM3 (38:1)
34.7	1237.8153	1237.8143	0.81	GM3 (40:1)
28.3	1384.8339	1384.8310	2.09	GM2 (36:1)
30.9	1412.8643	1412.8623	1.42	GM2 (38:1)
26.7	1546.8838	1546.8839	−0.06	GM1 (36:1)
30.2	1574.9177	1574.9152	1.02	GM1 (38:1)
23.5	1518.8539	1518.8526	0.86	GM1 (34:1)
24.3	1544.8697	1544.8695	1.59	GM1 (36:2)
27.6	1472.8486	1472.8471	0.13	GD3 (36:1)
26.2	1837.9846	1837.9793	2.88	GD1 (36:1)
28.4	1866.0087	1866.0106	−1.02	GD1 (38:1)

GM3 (34:1), (36:1), (38:1), and (40:1), two lipid forms of GM2 (36:1) and (38:1), and two lipid forms of GM1 (36:1) and (38:1) were readily discovered. However, the GM3 (42:1) lipid form observed in spiked plasma was not in the spiked brain, probably due to its low abundance in GM3 standard combined with lower spiking concentrations used for brain tissue. Interestingly, two other lipid forms of GM1 (34:1) and (36:2) that were not in spiked plasma were identified in the spiked brain. These forms of GM1 were probably endogenous for mouse brain. Moreover, analysis of the spiked mouse brain data using an in-lab GSL library containing the reference MS/MS spectra of GM1, GM2, GM3, GD1a/1b, GD2, GD3, and GB4 led to the identification of two other ganglioside species, GD3 and GD1, in varied lipid forms (Table 2), which were absent from spiked plasma. The reference MS/MS spectra of GD3 and GD1 and their different lipid forms, as well as product ions and signal intensities, are presented in the Supporting Information (Figures S8,S9 and Tables S4,S5). We verified later that these two gangliosides are also endogenous for the mouse brain.

The above results clearly suggest that the established extraction protocol can be used to effectively extract GSLs from brain tissues and that LC-MS/MS can be successfully used to analyze brain GSLs. This study also disclosed some endogenous gangliosides in the mouse brain.

https://doi.org/10.1021/acsomega.1c07070
ACS Omega 2022, 7, 6403−6411

Analysis of Mouse Brain. After the protocols and conditions for GSL extraction and LC-MS analysis were validated using the spiked mouse brain, we applied them to the study of gangliosides in the nonspiked mouse brain. Fresh mouse brain tissues were homogenized and extracted. The extracts were dried, reconstituted in methanol/chloroform, and applied to LC-MS/MS analysis. As described above, the two-stage matching of experimental LC-MS/MS spectra with the MS/MS spectra of our in-lab reference library was conducted to identify 10 gangliosides of 5 different species (Table 3). In addition to GD3 (36:1), GM1 (36:2) and (34:1), and GD1 (36:1) and (38:1) found in the spiked mouse brain, GM3 (36:1), GM2 (36:1) and (38:1), and GM1 (36:1) and (38:1) were also endogeneous in the mouse brain. Since the standards utilized to spike mouse brain were GM3, GM2, and GM1, they must have overlapped with endogeneous gangliosides during the analysis of the spiked mouse brain. The results of spiked and nonspiked mouse brains were consistent and corroborated with each other. Therefore, we had identified one GM3 lipid form, two GM2 lipid forms, four GM1 lipid forms, one GD3 lipid form, and two GD1 lipid forms as some major gangliosides in the mouse brain.

Table 3. Major Gangliosides Identified in Mouse and Human Brains

		mouse brain		human brain	
ganglioside	theoretical m/z	ID[a] in the sample	exp. mass deviation (ppm)	ID[a] in the sample	exp. mass deviation (ppm)
GM3 (36:1)	1181.7517	+	−1.95	+	−1.69
GM3 (38:1)	1209.7830	−		+	−1.49
GM3 (40:1)	1237.8143	−		+	−3.15
GM3 (42:2)	1263.8300	−		+	2.81
GM3 (42:1)	1265.8456	−		+	−2.05
GM2 (36:1)	1384.8310	+	−1.52	+	−1.22
GM2 (38:1)	1412.8623	+	−0.50	+	−0.07
GM1 (34:1)	1518.8526	+	−3.50	−	
GM1 (36:2)	1544.8695	+	−3.43	+	−0.39
GM1 (36:1)	1546.8839	+	−2.46	+	−1.81
GM1 (38:1)	1574.9152	+	−1.78	+	−0.95
GD3 (36:1)	1472.8471	+	0.07	+	−1.77
GD3 (38:1)	1500.8784	−		+	−1.13
GD2 (36:1)	1675.9265	−		+	−3.34
GD2 (38:1)	1703.9578	−		+	−1.12
GD1 (36:1)	1837.9793	+	−1.96	+	−0.27
GD1 (38:1)	1866.0106	+	−4.18	+	−1.07

[a]"+" and "−" indicate whether a specific ganglioside was identified or not in the mouse or human brain.

Analysis of Human Brain. After the successful analysis of gangliosides in the mouse brain, we tested the method for the human brain. Ganglioside extraction, LC-MS analysis, and two-stage MS/MS spectral matching followed the same protocols as for the mouse brain. The resulting MS/MS data were matched with our in-lab library of GSL MS/MS spectra to give results listed in Table 3. At least 16 gangliosides belonging to six species were identified, including five GM3 lipid forms, two GM2 lipid forms, three GM1 lipid forms, two GD3 lipid forms, two GD1 lipid forms, and two GD2 lipid forms (their MS spectra and product ions are presented in the Supporting Information, Figure S10 and Table S6). The experiments were replicated to obtain similar results for all 15 human brain samples (Supporting Information Table S7).

Discussion. Our study on ganglioside-spiked human plasma and mouse brain had shown that GSL extraction using a 3:4:2 mixture of water, methanol, and chloroform was effective for biological fluids and tissues because all were purposefully added and many endogenous gangliosides were successfully extracted from the matrix. It was also validated that analyzing the extracted gangliosides with LC-MS/MS followed by the two-stage matching of experimental and reference MS/MS spectra could identify both added and endogenous gangliosides. Repeating the experiments utilizing different brain tissues verified the overall consistency of the method. Therefore, the new method and its protocols can be used in confidence for the study of biological GSLs.

This study had also offered some interesting results about ganglioside constitutions in mouse and human brains. As indicated in Table 3, mouse and human brains have many gangliosides in common, but some gangliosides seem to be species- or region-specific. For example, two forms of GD2 (36:1) and (38:1) were found in the human brain sample but not in the whole mouse brain. GM3, GM2, GM1, GD3, and GD1 were present in human and mouse brains, but their lipid forms were different. We observed five forms of GM3 (36:1), (38:1), (40:1), (42:2), and (40:2) in the human brain but only GM3 (36:1) in the mouse brain. Similarly, for GD3, we found two lipid forms (36:1) and (38:1) in the human brain but only (36:1) in the mouse brain. In contrary, more GM1 lipid forms (34:1), (36:2), (36:1), and (38:1) were found in the mouse brain than in the human brain—(36:2), (36:1), and (38:1). Intriguingly, the GM1 (36:2) lipid form is not in LIPID MAPS,[50] a database encompassing structures and annotations of all biologically relevant lipids. Another interesting finding is that most gangliosides in both human and mouse brains carry mainly 36- and 38-carbon ceramides.

This work was mainly focused on methodology development and verification. Accepting that absolute GSL quantitation would not be accurate without labeled GSL internal standards, we can still perform relative quantitation. As ionization potentials and fragmentation patterns are similar for different lipid forms of a GSL, the integrated peak areas of their MS signals should quite accurately reflect the ratios of different lipid forms for each GSL species in the sample. The results in Figure 2A (Supporting Information, Table S9) clearly indicate that, in the mouse brain, the most abundant lipid for gangliosides is (36:1), followed by (38:1). For example, signals for the (36:1) form of GM2, GM1, and GD1 are several folds stronger than that of their corresponding (38:1) form. For GM3 and GD3, (36:1) is the only lipid form found, suggesting that even if GM3 and GD3 have other lipid forms, the abundance is too low to be detected. On the other hand, in the

https://doi.org/10.1021/acsomega.1c07070
ACS Omega 2022, 7, 6403−6411

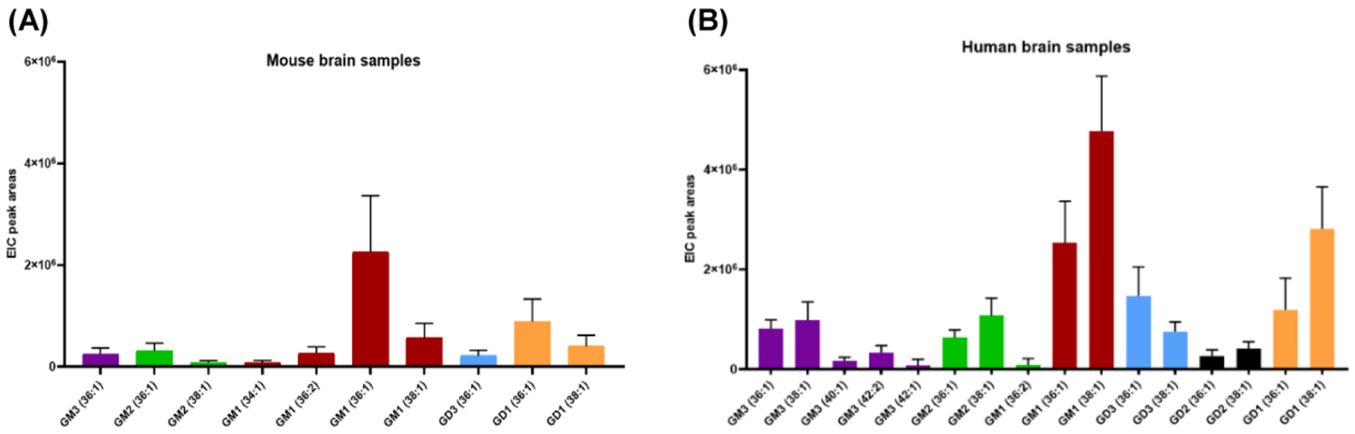

Figure 2. Extracted ion chromatogram (EIC) peak areas of the major gangliosides observed in mouse (A) and human (B) brain tissues.

human brain (Figure 2B and Supporting Information, Table S10), the most abundant lipid form for all gangliosides, except for GD3, is (38:1), followed by (36:1). Therefore, it seems that mouse and human have their preferred forms of ceramide.

Since all the above experiments were performed under the same extraction, LC and MS conditions, it is also feasible to estimate the relative quantities of various gangliosides in different brain tissues using the MS signal intensity. The data in Figure 2 indicate that mouse and human brains express overall different levels of gangliosides. For example, the signal intensities of most ganglioside species in the human brain were higher than those in the mouse brain. Considering that 25 mg of mouse brain tissue and 7 mg of human brain tissue were used in the experiments, after normalization, higher ganglioside expression levels in the human brain than in mouse brain would be even more significant.

In addition, a 1.0:0.94:0.56 ratio for the MS signals of GM3, GM2, and GM1 in a 1:1:1 mixture (molar, including all lipid forms) (Supporting Information Table S8) indicates that the MS signal and/or the extraction efficiency of GM1 are slightly lower than that of GM2 and GM3. On the other hand, these results also suggest that their differences are relatively small; thus, MS signal intensities may be utilized to roughly reflect the trend of changes in these gangliosides. Figure 2 shows that GM1 and GD1 are the most abundant gangliosides for both mouse and human brains, which are followed by GD3 and GM2. Since the MS signal and/or extraction efficiency of GM1 were lower than that of GM3 and GM2 under our experimental conditions, the high expression level of GM1 in these brains is probably even more impressive than that reflected by the signal intensities. Additionally, GD2 is identified in the human brain but not the whole mouse brain. However, we did not try to identify GT1b, another major brain ganglioside, in the samples since our library did not contain its reference MS/MS spectrum.

However, it should be noted that while mouse brain samples were taken from blended whole brains, human brain samples were derived from the dorsolateral prefrontal cortex. As brains are structurally complex and various regions can have different GSL profiles, the ganglioside levels of these human brain samples may not reflect whole human brain expression levels. To profile the overall expression levels and map the area distributions of gangliosides, whole-brain samples and tissues from different regions should be analyzed. On the other hand, our results of whole mouse brain are similar to that of the adult mouse cerebral cortex,[51] both having GM1 and GD1 as the most abundant gangliosides. Therefore, although detailed comparisons of mouse and human brains are more appropriate for the same areas, a brief comparison of mouse and human brain results obtained herein is justifiable and can provide some useful information. Nonetheless, current results do prove that the new analytical method can be used to identify various gangliosides or GSLs and their expression levels in brains. Moreover, the observation that mouse and human brains have different preferred lipid forms should be biologically significant as this is not likely limited to specific gangliosides or GSLs and local regions of the brain but correlated with the biosynthetic pathways of ceramide.

To perform absolute quantitation, it is necessary to add a labeled GSL standard (ideally one for each GSL species) to samples before extraction. This can avoid systemic errors caused by any variations in sample processing and differences in the GSL ionization potential. Another factor limiting extensive biological GSL analyses is the lack of a comprehensive database of MS/MS spectra due to difficult access to various GSL standards. Our in-lab database contains the MS/MS spectra of only a limited number of GSLs. Thus, this work was restricted by its scope and was only focused on gangliosides; we do not assume that the resultant GSL profiles of mouse and human brains are comprehensive. This will improve with continuous efforts to have more GSL standards and expand the library of reference GSL MS/MS spectra via such as more efficient synthesis of GSLs.[52,53]

Another challenge in GSL analysis is the identification of GSL isomers. According to the literature,[34,54] GSL anomeric and regio-isomers, such as GD1a and GD1b, can be separated and characterized by MS in combination with ultra-high-performance LC. However, GSL epimers, those differing for only one stereogenic center in a sugar unit, are still difficult to identify, and only the epimers of very simple GSLs were distinguished by IMS-MS.[54] Thus, IMS-MS should be a promising method for GSL isomer analysis.[55−57] As our GD1 standard was a mixture and GSL isomer identification is a problem needing additional attention, whereas the main focus of this work is method validation, we did not spend much effort to conduct an in-depth analysis of isomers such as GD1a and GD1b in these samples. However, we believe that in combination with ultra-high-resolution LC or IMS-MS our method should be at least as efficient as previously reported methods for anomeric and regio-isomer identification.

In addition, currently, there is no software especially created for two-stage MS-based GSL identification. The existing

https://doi.org/10.1021/acsomega.1c07070
ACS Omega 2022, 7, 6403−6411

software for MS-based glycomics and lipidomics analysis has limitations and alone fail to identify many GSLs. For example, analyzing the mouse brain data using SimLipid (Premier Biosoft Int., v.6.05) produced six positive identifications, including GM3 (36:1), GM2 (36:1), GM1 (36:1), GD3 (36:1), GD1 (36:1), and (38:1), opposed to 10−16 gangliosides identified with the two-stage matching method. LipidBlast (v.66), a rule-based lipid library, was also tested, but the search did not result in any ganglioside annotation in the mouse brain. Nonetheless, the existing software did accelerate our two-stage matching process through quick identification of precursor ions. These results have not only verified the advantages of the two-stage MS spectral matching method for GSL analysis in biological tissues but also indicated the demand for software for two-stage MS/MS spectral matching to allow for more effective GSL identification.

CONCLUSIONS

In summary, we have established and verified herein the practical protocols for GSL extraction from plasma and brain tissues and for LC-MS/MS analysis of the extracted GSLs, using defined samples spiked with ganglioside standards. The two-stage MS/MS spectral matching method was proved to be able to characterize all spiked gangliosides including various lipid forms. Therefore, this work has built a solid foundation for the method to be applied to the study of biological gangliosides. Although this work is focused on gangliosides due to the limitations of available GSL standards and reference MS/MS spectra, the method should be applicable to other gangliosides and GSLs as well, since the positive ionization mode used in this work is also widely applicable to neutral GSLs. However, if only gangliosides are studied, this method may be more sensitive using the negative ionization mode as gangliosides, especially highly sialylated ones like GT1b, which can be more easily ionized under negative ionization conditions. Subsequently, the method and its protocols were used to identify gangliosides in mouse and human brains. These studies have provided some useful information about the ganglioside profiles of the mouse brain and the dorsolateral prefrontal cortex of the human brain. Whereas mouse and human brains show some differences in ganglioside compositions, both have GM1 and GD1 and then GD3 and GM2 in various lipid forms as the major gangliosides, which agrees with previous reports.[51,58,59] An important feature of this new method is that the characterization of various GSL lipid forms does not rely on their LC profiles, which is different from previously reported methods.[34,54] This can avoid uncertainties caused by the variations in LC conditions, thereby rendering the new method reliable and generally applicable. Intriguingly, we find that mouse and human brain gangliosides have different predominant lipid forms. While the new method for biological GSL identification was proved accurate and effective, it is limited by the lack of an extensive database of reference GSL MS/MS spectra and software especially designed to perform the two-stage matching of experimental and reference MS/MS spectra. If these issues are solved, the method can be more powerful for truly high-throughput glycolipidomics analysis. Currently, our laboratories are working on expanding the GSL MS/MS spectra library and developing the suitable software.

EXPERIMENTAL METHODS

Materials. LC-MS grade acetonitrile, isopropanol, formic acid, methanol, and water and ACS grade chloroform and ammonium formate were purchased from Fisher Scientific. GM3, GM2, and GM1 standards derived from porcine brains were purchased from Avanti Polar Lipids. Each standard was dissolved in methanol to generate an individual stock solution (1.0 mg/mL). The stock solutions of GM3, GM2, and GM1 (10 μL each) were added in 970 μL of methanol to obtain a mixture of standards with a concentration of 10 μg/mL for each ganglioside. Human plasma samples were purchased from Innovative Research Inc. with K3 EDTA as the anticoagulant. Mouse brains were extracted from euthanized mice (Jackson Laboratory), and the animal use protocol was approved by the Institutional Animal Care and Use Committee (IACUC) of the University of Florida. Human postmortem brain tissues were obtained from the Rush Alzheimer's Disease Center at Rush University Medical Center. Human tissues were deidentified, and their use met the requirement of Exemption 4.

GSL Extraction from Plasma. To a plasma sample (50 μL) was added above GSL standard mixture (30 μL), and the sample was shaken vigorously. Then, a mixture of water, methanol, and chloroform (3:4:2, v/v/v; 1800 μL) was added, followed by vortexing (1 min). After the sample was incubated at −20 °C for 2 h and centrifuged at 1000*g* for 20 min, the top layer was transferred into a glass vial, and the remaining was extracted again with the same solvent (900 μL) in the same manner. The combined top layer was condensed on a SpeedVac Concentrator, and the residue was reconstituted in methanol containing 1% chloroform (150 μL) for LC-MS/MS analysis.

Extraction of GSLs from the Brain. The same protocol was used for GSL extraction from the spiked mouse brain and nonspiked mouse and human brains. Blended mouse brain tissues (25 mg) with or without standard GSL spikes (5 μL) and human brain samples (7 mg) from the dorsolateral prefrontal cortex were mixed with water (600 μL) in a tube filled with triple-pure high impact zirconium beads (1.5 mm). This mixture was homogenized at 300× speed 30 times (30 s each time) on a BeadBug microtube homogenizer. Then, the sample was transferred into a centrifuge tube, followed by adding methanol (800 μL) and chloroform (400 μL). The mixture was vortexed for 1 min, chilled at −20 °C for 2 h, and centrifuged for 20 min. The top layer was transferred into a glass vial. The remaining was extracted again with the same mixture of solvents (900 μL). The combined top layer was dried, and the residue was reconstituted in methanol containing 1% chloroform (150 μL) for LC-MS/MS analysis.

LC-MS Analysis. Each of the reconstituted GSL samples from human plasma and the mouse brain (5 μL/injection) or the human brain (2−4 μL/injection, based on normalized protein content) was injected in a Thermo Fischer Scientific UltiMate 3000 RSLCnano system equipped with an Acclaim PepMap RSLC C18 column (300 μm × 15 cm, 2 μm, 100 Å) and a precolumn (3 mm × 2 cm, 75 μm, 100 Å). The autosampler and columns were kept at temperatures of 4 and 40 °C, respectively, during the analysis. Samples loaded to the precolumn were washed for 5 min with 98/2% water/acetonitrile containing 0.1% formic acid at a 25 μL/min flow rate. For LC, mobile phases, (A) acetonitrile/water 60/40% and (B) isopropanol/acetonitrile/water 90/8/2% both con-

https://doi.org/10.1021/acsomega.1c07070
ACS Omega 2022, 7, 6403−6411

taining 10 mM ammonium formate and 0.1% formic acid were used for the gradient pump at a 5 μL/min flow rate. The mobile-phase gradient was 50% B for 5 min, ramping to 75% B at 50 min, and to 98% B at 70 min. The gradient was held at 98% B for 20 min before returning to 50% B in 5 min. MS conditions were as follows. An Impact II QqTOF mass spectrometer (Bruker Daltonics) was used to acquire MS or MS/MS spectra, utilizing Apollo electrospray ionization (ESI) operated in a positive mode with a capillary voltage of 4.0 kV, nebulizing gas pressure of 0.3 bar, dry nitrogen gas flow 4.0 L/min, and drying gas temperature of 200 °C. The instrument was programmed for data-dependent acquisition (DDA) for CID using a nitrogen collision gas partner. DDA was selected for singly and doubly charged ions in a mass range of m/z 500−2000 using an m/z 2 mass window. The collision energies used for fragmentations were between 25 and 40 eV, depending on the programmed mass bracket. The active exclusion was employed to exclude an ion after the acquisition of a single spectrum for 3 min unless the current-to-previous intensity ratio was greater than or equal to 2.0.

■ ASSOCIATED CONTENT

Supporting Information

The Supporting Information is available free of charge at https://pubs.acs.org/doi/10.1021/acsomega.1c07070.

Product spectra of various lipid forms of GM3, GM2, GM1, GD3, GD2, and GD1, tables of the matched product ions and their fragment assignments, tables of various lipid forms of gangliosides identified in the human brain, tables of the integrated EIC signals of various gangliosides in mouse and human brains, and the EICs of LC-MS/MS (PDF)

■ AUTHOR INFORMATION

Corresponding Author

Zhongwu Guo − *Department of Chemistry, University of Florida, Gainesville, Florida 32611, United States;* orcid.org/0000-0001-5302-6456; Email: zguo@chem.ufl.edu

Authors

Fanran Huang − *Department of Chemistry, University of Florida, Gainesville, Florida 32611, United States*

Laura S. Bailey − *Department of Chemistry, University of Florida, Gainesville, Florida 32611, United States*

Tianqi Gao − *Department of Chemistry, University of Florida, Gainesville, Florida 32611, United States*

Wenjie Jiang − *Department of Chemistry, University of Florida, Gainesville, Florida 32611, United States*

Lei Yu − *Rush Alzheimer's Disease Center, Rush University Medical Center, Chicago, Illinois 60612, United States*

David A. Bennett − *Rush Alzheimer's Disease Center, Rush University Medical Center, Chicago, Illinois 60612, United States*

Jinying Zhao − *Department of Epidemiology, University of Florida, Gainesville, Florida 32611, United States*

Kari B. Basso − *Department of Chemistry, University of Florida, Gainesville, Florida 32611, United States*

Complete contact information is available at: https://pubs.acs.org/10.1021/acsomega.1c07070

Notes

This work followed the general practice and standards about research ethics and does not have any significant hazards or risks to perform.

The authors declare no competing financial interest.

■ ACKNOWLEDGMENTS

This work is partly supported by an NSF grant (CHE-1800279) to ZG. ZG is grateful to Steven and Rebecca Scott for the endowment. The MS instrument was funded by NIH (S10 OD021758).

■ REFERENCES

(1) Stults, C. L. M.; Sweeley, C. C.; Macher, B. A. Glycosphingolipids: Structure, biological source, and properties. *Methods in Enzymology*; Academic Press, 1989; Vol. *179*, pp 167−214.

(2) Merrill, A. H. Sphingolipid and glycosphingolipid metabolic pathways in the era of sphingolipidomics. *Chem. Rev.* **2011**, *111*, 6387−6422.

(3) Vukelic, Z.; Metelmann, W.; Müthing, J.; Kos, M.; Peter-Katalinic, J. Anencephaly: Structural characterization of gangliosides in defined brain regions. *Biol. Chem.* **2001**, *382*, 259−274.

(4) Schnaar, R. L.; Gerardy-Schahn, R.; Hildebrandt, H. Sialic Acids in the Brain: Gangliosides and polysialic acid in nervous system development, stability, disease, and regeneration. *Physiol. Rev.* **2014**, *94*, 461−518.

(5) Posse de Chaves, E.; Sipione, S. Sphingolipids and gangliosides of the nervous system in membrane function and dysfunction. *FEBS Lett.* **2010**, *584*, 1748−1759.

(6) Russo, D.; Parashuraman, S.; D'Angelo, G. Glycosphingolipid−protein interaction in signal transduction. *Int. J. Mol. Sci.* **2016**, *17*, No. 1732.

(7) Sonnino, S.; Mauri, L.; Ciampa, M. G.; Prinetti, A. Gangliosides as regulators of cell signaling: ganglioside-protein interactions or ganglioside-driven membrane organization? *J. Neurochem.* **2013**, *124*, 432−435.

(8) Sonnino, S.; Mauri, L.; Chigorno, V.; Prinetti, A. Gangliosides as components of lipid membrane domains. *Glycobiology* **2007**, *17*, 1R−13R.

(9) Lopez, P. H. H.; Schnaar, R. L. Gangliosides in cell recognition and membrane protein regulation. *Curr. Opin. Struct. Biol.* **2009**, *19*, 549−557.

(10) Hakomori, S. Bifunctional role of glycosphingolipids. Modulators for transmembrane signaling and mediators for cellular interactions. *J. Biol. Chem.* **1990**, *265*, 18713−18716.

(11) Hakomori, S.-I.; Handa, K. GM3 and cancer. *Glycoconj. J.* **2015**, *32*, 1−8.

(12) Lingwood, C. A. Glycosphingolipid functions. *Cold Spring Harb. Perspect. Biol.* **2011**, *3*, No. a004788.

(13) D'Angelo, G.; Capasso, S.; Sticco, L.; Russo, D. Glycosphingolipids: Synthesis and functions. *FEBS J.* **2013**, *280*, 6338−6353.

(14) Wennekes, T.; van den Berg, R. J. B. H. N.; Boot, R. G.; van der Marel, G. A.; Overkleeft, H. S.; Aerts, J. M. F. G. Glycosphingolipids—Nature, function, and pharmacological modulation. *Angew. Chem., Int. Ed.* **2009**, *48*, 8848−8869.

(15) Vukelić, e.; Kalanj-Bognar, S.; Froesch, M.; Bîndilă, L.; Radić, B.; Allen, M.; Peter-Katalinić, J.; Zamfir, A. D. Human gliosarcoma-associated ganglioside composition is complex and distinctive as evidenced by high-performance mass spectrometric determination and structural characterization. *Glycobiology* **2007**, *17*, 504−515.

(16) Park, D. D.; Xu, G.; Wong, M.; Phoomak, C.; Liu, M.; Haigh, N. E.; Wongkham, S.; Yang, P.; Maverakis, E.; Lebrilla, C. B. Membrane glycomics reveal heterogeneity and quantitative distribution of cell surface sialylation. *Chem. Sci.* **2018**, *9*, 6271−6285.

(17) van Echten-Deckert, G.; Walter, J. Sphingolipids: Critical players in Alzheimer's disease. *Prog. Lipid Res.* **2012**, *51*, 378−393.

(18) Ariga, T.; Wakade, C.; Yu, R. K. The pathological roles of ganglioside metabolism in Alzheimer's disease: Effects of gangliosides on neurogenesis. *Int. J. Alzheimers Dis.* **2011**, *2011*, No. e193618.
(19) Sayre, L. M.; Zelasko, D. A.; Harris, P. L. R.; Perry, G.; Salomon, R. G.; Smith, M. A. 4-Hydroxynonenal-derived advanced lipid peroxidation end products are increased in Alzheimer's disease. *J. Neurochem.* **1997**, *68*, 2092−2097.
(20) Markesbery, W. R.; Kryscio, R. J.; Lovell, M. A.; Morrow, J. D. Lipid peroxidation is an early event in the brain in amnestic mild cognitive impairment. *Ann. Neurol.* **2005**, *58*, 730−735.
(21) Gu, F.; Zhu, M.; Shi, J.; Hu, Y.; Zhao, Z. Enhanced oxidative stress is an early event during development of Alzheimer-like pathologies in presenilin conditional knock-out mice. *Neurosci. Lett.* **2008**, *440*, 44−48.
(22) Kaida, K.; Ariga, T.; Yu, R. K. Antiganglioside antibodies and their pathophysiological effects on Guillain−Barré syndrome and related disorders—A review. *Glycobiology* **2009**, *19*, 676−692.
(23) Yuki, N. Guillain-Barre syndrome and anti-ganglioside antibodies: A clinician-scientist's journey. *Proc. Jap. Acad., Series B* **2012**, *88*, 299−326.
(24) Shaner, R. L.; Allegood, J. C.; Park, H.; Wang, E.; Kelly, S.; Haynes, C. A.; Sullards, M. C.; Merrill, A. H. Quantitative analysis of sphingolipids for lipidomics using triple quadrupole and quadrupole linear ion trap mass spectrometers. *J. Lipid Res.* **2009**, *50*, 1692−1707.
(25) Li, M.; Tong, X.; Lv, P.; Feng, B.; Yang, L.; Wu, Z.; Cui, X.; Bai, Y.; Huang, Y.; Liu, H. A not-stop-flow online normal-/reversed-phase two-dimensional liquid chromatography−quadrupole time-of-flight mass spectrometry method for comprehensive lipid profiling of human plasma from atherosclerosis patients. *J. Chromatogr. A* **2014**, *1372*, 110−119.
(26) Boutin, M.; Menkovic, I.; Martineau, T.; Vaillancourt-Lavigueur, V.; Toupin, A.; Auray-Blais, C. Separation and analysis of lactosylceramide, galabiosylceramide, and globotriaosylceramide by LC-MS/MS in urine of Fabry disease patients. *Anal. Chem.* **2017**, *89*, 13382−13390.
(27) Lee, H.; Lerno, L. A.; Choe, Y.; Chu, C. S.; Gillies, L. A.; Grimm, R.; Lebrilla, C. B.; German, J. B. Multiple precursor ion scanning of gangliosides and sulfatides with a reversed-phase microfluidic chip and quadrupole time-of-flight mass spectrometry. *Anal. Chem.* **2012**, *84*, 5905−5912.
(28) Ikeda, K.; Shimizu, T.; Taguchi, R. Targeted analysis of ganglioside and sulfatide molecular species by LC/ESI-MS/MS with theoretically expanded multiple reaction monitoring. *J. Lipid Res.* **2008**, *49*, 2678−2689.
(29) Sørensen, L. K. A liquid chromatography/tandem mass spectrometric approach for the determination of gangliosides GD3 and GM3 in bovine milk and infant formulae. Rapid Commun. *Mass Spectrom.* **2006**, *20*, 3625−3633.
(30) Li, Q.; Sun, M.; Yu, M.; Fu, Q.; Jiang, H.; Yu, G.; Li, G. Gangliosides profiling in serum of breast cancer patient: GM3 as a potential diagnostic biomarker. *Glycoconj. J.* **2019**, *36*, 419−428.
(31) Polo, G.; Burlina, A. P.; Kolamunnage, T. B.; Zampieri, M.; Dionisi-Vici, C.; Strisciuglio, P.; Zaninotto, M.; Plebani, M.; Burlina, A. B. Diagnosis of sphingolipidoses: a new simultaneous measurement of lysosphingolipids by LC-MS/MS. *Clin. Chem. Lab. Med.* **2017**, *55*, 403−414.
(32) Kirsch, S.; Zarei, M.; Cindrić, M.; Müthing, J.; Bindila, L.; Peter-Katalinić, J. On-line nano-HPLC/ESI QTOF MS and tandem MS for separation, detection, and structural elucidation of human erythrocytes neutral glycosphingolipid mixture. *Anal. Chem.* **2008**, *80*, 4711−4722.
(33) Lavoie, P.; Boutin, M.; Auray-Blais, C. Multiplex analysis of novel urinary Lyso-Gb3-related biomarkers for Fabry disease by tandem mass spectrometry. *Anal. Chem.* **2013**, *85*, 1743−1752.
(34) Hájek, R.; Jirásko, R.; Lísa, M.; Cífková, E.; Holčapek, M. Hydrophilic interaction liquid chromatography−Mass spectrometry characterization of gangliosides in biological samples. *Anal. Chem.* **2017**, *89*, 12425−12432.
(35) Ikeda, K.; Taguchi, R. Highly sensitive localization analysis of gangliosides and sulfatides including structural isomers in mouse cerebellum sections by combination of laser microdissection and hydrophilic interaction liquid chromatography/electrospray ionization mass spectrometry with theoretically expanded multiple reaction monitoring. *Rapid Commun. Mass Spectrom.* **2010**, *24*, 2957−2965.
(36) Almeida, R.; Mosoarca, C.; Chirita, M.; Udrescu, V.; Dinca, N.; Vukelić, Ž.; Allen, M.; Zamfir, A. D. Coupling of fully automated chip-based electrospray ionization to high-capacity ion trap mass spectrometer for ganglioside analysis. *Anal. Biochem.* **2008**, *378*, 43−52.
(37) Serb, A. F.; Sisu, E.; Vukelić, Ž.; Zamfir, A. D. Profiling and sequencing of gangliosides from human caudate nucleus by chip-nanoelectrospray mass spectrometry. *J. Mass Spectrom.* **2012**, *47*, 1561−1570.
(38) Fabris, D.; Rožman, M.; Sajko, T.; Vukelić, Ž. Aberrant ganglioside composition in glioblastoma multiforme and peritumoral tissue: A mass spectrometry characterization. *Biochimie* **2017**, *137*, 56−68.
(39) Sarbu, M.; Clemmer, D. E.; Zamfir, A. D. Ion mobility mass spectrometry of human melanoma gangliosides. *Biochimie* **2020**, *177*, 226−237.
(40) Sarbu, M.; Vukelić, Ž.; Clemmer, D. E.; Zamfir, A. D. Ion mobility mass spectrometry provides novel insights into the expression and structure of gangliosides in the normal adult human hippocampus. *Analyst* **2018**, *143*, 5234−5246.
(41) Bou Khalil, M.; Hou, W.; Zhou, H.; Elisma, F.; Swayne, L. A.; Blanchard, A. P.; Yao, Z.; Bennett, S. A. L.; Figeys, D. Lipidomics era: Accomplishments and challenges. *Mass Spectrom. Rev.* **2010**, *29*, 877−929.
(42) Farwanah, H.; Kolter, T. Lipidomics of glycosphingolipids. *Metabolites* **2012**, *2*, 134−164.
(43) Tissot, B.; North, S. J.; Ceroni, A.; Pang, P.-C.; Panico, M.; Rosati, F.; Capone, A.; Haslam, S. M.; Dell, A.; Morris, H. R. Glycoproteomics: Past, present and future. *FEBS Lett.* **2009**, *583*, 1728−1735.
(44) Bailey, L. S.; Huang, F.; Gao, T.; Zhao, J.; Basso, K. B.; Guo, Z. Characterization of glycosphingolipids and their diverse lipid forms through two-stage matching of LC-MS/MS spectra. *Anal. Chem.* **2021**, *93*, 3154−3162.
(45) Domon, B.; Costello, C. E. A systematic nomenclature for carbohydrate fragmentations in FAB-MS/MS spectra of glycoconjugates. *Glycoconj. J.* **1988**, *5*, 397−409.
(46) Kind, T.; Liu, K.-H.; Lee, D. Y.; DeFelice, B.; Meissen, J. K.; Fiehn, O. LipidBlast in silico tandem mass spectrometry database for lipid identification. *Nat. Methods* **2013**, *10*, 755−758.
(47) Koelmel, J. P.; Kroeger, N. M.; Ulmer, C. Z.; Bowden, J. A.; Patterson, R. E.; Cochran, J. A.; Beecher, C. W. W.; Garrett, T. J.; Yost, R. A. LipidMatch: An automated workflow for rule-based lipid identification using untargeted high-resolution tandem mass spectrometry data. *BMC Bioinformatics* **2017**, *18*, No. e331.
(48) Kind, T.; Okazaki, Y.; Saito, K.; Fiehn, O. LipidBlast templates as flexible tools for creating new in-Silico tandem mass spectral libraries. *Anal. Chem.* **2014**, *86*, 11024−11027.
(49) Svennerholm, L.; Fredman, P. A procedure for the quantitative isolation of brain gangliosides. *Biochim. Biophys. Acta* **1980**, *617*, 97−109.
(50) Sud, M.; Fahy, E.; Cotter, D.; Brown, A.; Dennis, E. A.; Glass, C. K.; Merrill, A. H.; Jr; Murphy, R. C.; Raetz, C. R. H.; Russell, D. W.; Subramaniam, S. LMSD: LIPID MAPS structure database. *Nucleic Acids Res.* **2007**, *35*, D527−D532.
(51) Seyfried, T. N.; Yu, R. K.; Saito, M.; Albert, M. Ganglioside composition of an experimental mouse brain tumor. *Cancer Res.* **1987**, *47*, 3538−3542.
(52) Rohokale, R. S.; Li, Q.; Guo, Z. A Diversity-oriented strategy for chemical synthesis of glycosphingolipids: Synthesis of glycosphingolipid LcGg4 and its analogues and derivatives. *J. Org. Chem.* **2021**, *86*, 1633−1648.

https://doi.org/10.1021/acsomega.1c07070
ACS Omega 2022, 7, 6403−6411

(53) Li, Q.; Jaiswal, M.; Rohokale, R. S.; Guo, Z. A Diversity-oriented strategy for chemoenzymatic synthesis of glycosphingolipids and related derivatives. *Org. Lett.* **2020**, *22*, 8245−8249.
(54) Hu, T.; Jia, Z.; Zhang, J. Strategy for comprehensive profiling and identification of acidic glycosphingolipids using ultra-high-performance liquid chromatography coupled with quadrupole time-of-flight mass spectrometry,. *Anal. Chem.* **2017**, *89*, 7808−7816.
(55) Hofmann, J.; Hahm, H. S.; Seeberger, P. H.; Pagel, K. Identification of carbohydrate anomers using ion mobility−mass spectrometry. *Nature* **2015**, *526*, 241−244.
(56) Wojcik, R.; Webb, I. K.; Deng, L.; Garimella, S. V. B.; Prost, S. A.; Ibrahim, Y. M.; Baker, E. S.; Smith, R. D. Lipid and glycolipid isomer analyses using ultra-high resolution ion mobility spectrometry separations. *Int. J. Mol. Sci.* **2017**, *18*, No. e183.
(57) Masellis, C.; Khanal, N.; Kamrath, M. Z.; Clemmer, D. E.; Rizzo, T. R. Cryogenic vibrational spectroscopy provides unique fingerprints for glycan identification. *J. Am. Soc. Mass Spectrom.* **2017**, *28*, 2217−2222.
(58) Baek, R. C.; Martin, D. R.; Cox, N. R.; Seyfried, T. N. Comparative analysis of brain lipids in mice, cats, and humans with Sandhoff disease. *Lipids* **2009**, *44*, 197−205.
(59) Zarei, M.; Bindila, L.; Souady, J.; Dreisewerd, K.; Berkenkamp, S.; Muthing, J.; Peter-Katalinic, J. A sialylation study of mouse brain gangliosides by MALDI a-TOF and o-TOF mass spectrometry. *J. Mass Spectrom.* **2008**, *43*, 716−725.

https://doi.org/10.1021/acsomega.1c07070
ACS Omega 2022, 7, 6403−6411